Reflecting Ablating Heat Shields for Planetary Entry

DAVID L. PETERSON,* PHILIP R. NACHTSHEIM,† AND JOHN T. HOWE*
NASA Ames Research Center, Moffett Field, Calif.

Heat shielding for planetary entry probes of future Jovian and Venusian missions will encounter heating levels well beyond those previously experienced. These entries are typically dominated by radiative heating from the shock layer. This paper demonstrates the potential reflecting this incident radiation diffusely from an ablating material. This technique contrasts with the absorption experienced by char-forming or graphitic ablators. Two dielectric materials, Teflon (polytetrafluoroethylene) and boron nitride, are examined for their ablative performance, including reflection, in a combined convective and radiative heating environment. For Teflon, at the conditions obtained, superimposition of radiative heating upon a convective stream causes no additional increase in surface recession over the convective results. For boron nitride, an excellent room-temperature reflector in the visible spectrum, a decrease in reflectivity from 90% to 55% is experienced when the surface undergoes sublimation at high temperatures. The process of reflection in each of these materials is described in terms of backscattering from crystals. The significance of a sizable reflection as a mode of energy accommodation is demonstrated for Venusian and Jovian entries as a potential reduction in mass loss due to ablation.

Introduction

PLANETARY explorer missions have been proposed for Jupiter and Venus. Probes entering these planetary atmospheres will require heat shielding capable of withstanding convective and radiative heating environments much more severe than current experience. Lightweight insulative materials were developed to protect the entry body during the Apollo era of heat shield design. These materials were generally carbonaceous and usually formed a char layer of nearly pure carbon. For the levels of heating of interest for Apollo (about 1 kw/cm^2 peak heating rate in radiation or convection) the high-temperature black char acts as an exceedingly advantageous energy accommodation mechanism because of reradiation of energy. Today, heat shield design philosophy is still generally pervaded by the black surface concept although the entry requirements of planetary missions have been shifted to much more severe levels dominated by radiation heating.

One direction emphasized is use of graphitic materials that can accommodate more energy by other processes. For the Jovian entry case with heating fluxes in the 10-20 kw/cm^2 range, the high intrinsic heat of ablation of graphite and the blockage of radiation from the shock layer by the sublimation species in the boundary layer[1] are dominant modes of accommodation to the environment. Reradiation now plays a secondary role because of an upper limit of 1.8 kw/cm^2 even though the surface is taken to be near the triple point for carbon (4200°K) and is a black body. The entry histories for Jupiter and Venus are, however, dominated by radiation heating and of a magnitude well in excess of 1.8 kw/cm^2, on the order of 15kw/cm^2 (Refs. 2 and 3). Graphite, a very strong absorber, must then achieve the other modes of energy accommodation described here.

The predominance of radiative heating during entry dictates a different approach to heat shield design. This fact was pointed out by several people, including Allen in 1962 (Ref. 4). He suggested a heat shield concept that would act as a mirror and reflect the radiation away from the vehicle. His scheme consisted of introducing small oriented metallic flakes of high reflectivity into a base material of high transparency. The technique investigated herein, which was initially described in Ref. 5, utilizes "white" dielectic materials that reflect the radiation diffusely rather than specularly as with metallic flakes. The process by which this diffuse reflection is accomplished by internal refractions and reflections is reviewed in the next section.

The important practical problem is to provide a material that maintains reflection even while undergoing ablation. Although a hybrid system of flakes and binder may have good reflective properties, absorption always accompanies reflection at a metallic reflector; for trapped radiation, the heat shield will be strongly absorptive because of multiple reflections. Dielectric materials may be selected, by contrast, to achieve negligible absorption in a certain spectral range and also maintain good reflectivity. The purpose of this study is to illustrate the potential of a reflecting heat shield by demonstrating, with a combined convective and radiative heating test environment, the ablation performance of two dielectric heat shield materials that exhibit diffuse reflectance. The significance of the reflecting ablator concept is illustrated by calculating the mass loss for Venusian and Jovian entries for the dielectics.

Reflection Principle

Reflection from a dielectric body is accomplished by internal reflections and refractions. A "white" dielectric is composed of crystalline sites that have an index of refraction different from the surrounding medium or binder. This difference results in partial reflection of incident radiation at each boundary between crystal and binder. The reflected component is returned through the surface and the remaining portion is refracted into the crystal. Each crystallite, or reflection site, thus sets up a system of scattered radiation composed of reflected, or backscattered, radiation and refracted, or forward-scattered, radiation. The relative effectiveness of the scattering for reflective purposes is a consequence of the inherent optical properties of the crystallite, e.g., index of refraction, crystal size, absorption index and crystal shape.[6] In the absence of significant absorption, the radiation is reflected uniformly, especially in the visible spectrum, regardless of the wavelength. This reflection results in a "white" appearance and is identical to the process of reflection in white paints and coatings.[7] In that case, the paint is composed of a colorless transparent pigment (e.g., titanium dioxide or zinc oxide) suspended in a colorless base liquid, or "vehicle." Each of the pigment particles acts as a scattering site; the large number of scattering centers results in efficient radiation reflection. The white color is not due to suspending "white" particles in the

Presented as Paper 72-89 at the AIAA 10th Aerospace Sciences Meeting, San Diego, Calif., January 17–19, 1972; submitted January 31, 1972; revision received June 8, 1972. The authors gratefully acknowledge the assistance of R. M. Wakefield in the calculation of mass transfer for boron nitride.

Index categories: Unmanned Lunar and Interplanetary Systems; Material Ablation: Radiation and Radiative Heat Transfer.

* Research Scientist.

† Research Scientist. Member AIAA.

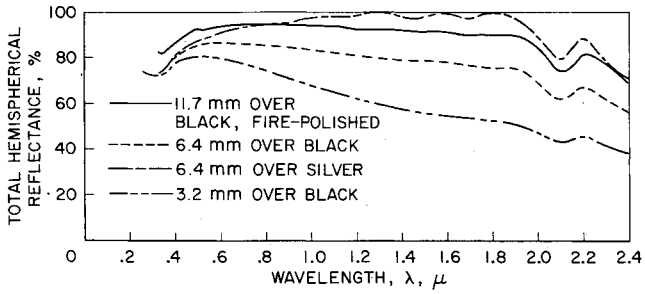

Fig. 1 Spectral reflectance for Teflon at room temperature.

binder, but is simply a consequence of the difference in index of refraction between binder and pigment.

Reflection Processes for Teflon and Boron Nitride

Teflon (polytetrafluoroethylene) and boron nitride were used in this investigation to demonstrate the principle of diffuse reflectance by a dielectric. These materials differ widely in their thermochemical characteristics and optical properties. Teflon, a polymer, is essentially a low temperature sublimer whereas boron nitride is a sintered crystalline, very similar to graphite, and sublimes at a relatively high temperature.

Reflection in Teflon is accomplished by volume scattering using a relatively deep zone of material[5] as will be shown below. Teflon is a polycrystalline material with the crystallite and adjacent amorphous zones uniformly distributed.[8] The difference in index of refraction between the amorphous "binder" and the microcrystallites results in reflections and refractions at the boundaries of these two zones. Incident radiation at each crystallite forms a scattering distribution (lobes) characterized by a relatively weak backscattering pattern and strong forward scattering. The backscattered lobes of radiation are additive, however, in reflection because of the very weak absorption and the large forward scattering lobes seen upon return to the body first surface. As a result, increasing the thickness of Teflon increases the over-all reflectance (Fig. 1). This figure shows the total hemispherical spectral reflectance of different thicknesses of Teflon backed by either a black surface or a highly reflective surface. The measurements were obtained in an integrating sphere reflectometer.[9] At the near ultraviolet end of the spectrum, the reflectance curves tend to approach a constant value of about 73%, which indicates the presence of absorption as well as a short optical depth for ultraviolet. At these shorter wavelengths the radiation is reflected in less depth probably because of the gain in the backscatter direction as a result of the larger particle size to wavelength ratio (Ref. 6). The fire-polished surface of a sample 11.7 mm thick shows the greatest effect in the ultraviolet with an increase in total reflectance.

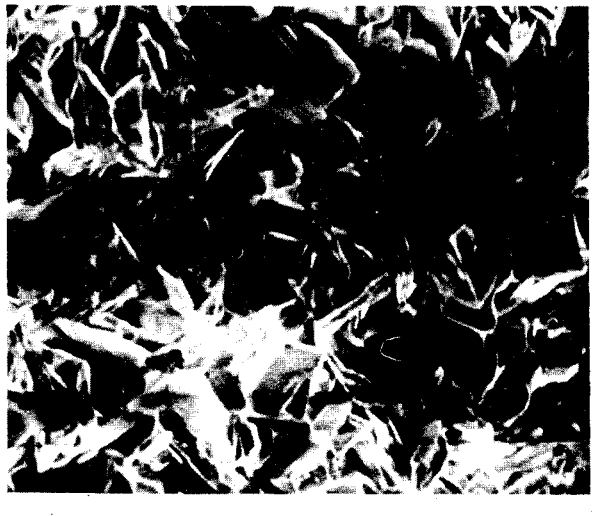

Fig. 2 Boron nitride solid at 1600× magnification using a scanning electron microscope.

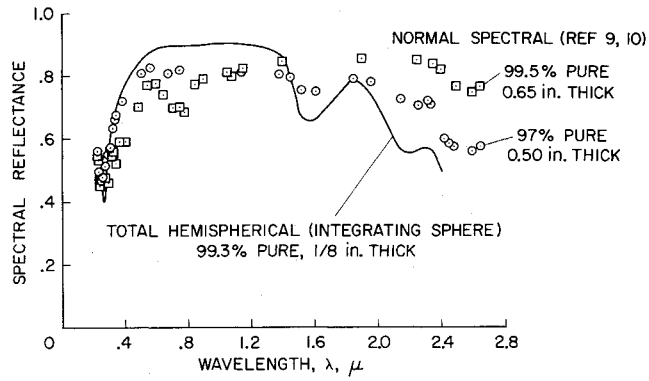

Fig. 3 Spectral reflectance for boron nitride at room temperature.

For radiation in the near infrared region, the crystallities have a lower backscattering efficiency but also a very low absorption coefficient. The effect of increasing the thickness is most pronounced in this region. In addition, backing the 6.4 mm sample with a highly reflective silver surface increases the reflectance to nearly 100% in the infrared but does not affect the ultraviolet and visible portion significantly because that radiation has already been either backscattered or absorbed. In the infrared region, the crystallites have less effect on the radiation with likely dissymmetry toward forward scattering. Although the backscatter lobes are small, they are additive in depth and lead to improved reflectance with thickness.

The crystallites in Teflon are formed by polymer chains fitted into a close-packed ordered arrangement. When Teflon is heated above 327°C, the crystallite chains become disordered (melt) and the substance becomes transparent to at least the visible spectrum. Below 327°C, the crystallites remain and are responsible for the volume reflection described previously.

In contrast, solid boron nitride is formed by hot-pressing and sintering boron nitride crystals, which are flat platelets, much like graphite, with hexagonal crystal structure (Fig. 2). The total hemispherical spectral reflectance of boron nitride at room temperature is shown in Fig. 3. The reflectance was obtained in the same reflectometer mentioned previously. Only a single thickness is shown since boron nitride has a much shorter photon mean free path than Teflon. The reflection from boron nitride is accomplished near the surface. The backscattering efficiency of boron nitride crystals is typically higher than Teflon crystallites. Also shown on Fig. 3 is published data on normal spectral reflectance of boron nitride.[10] An absorption edge appears in the 0.3 μ region but is accompanied by a slight recovery at about 0.23 μ. Data below 0.23 μ is not available but the reflectance is expected to fall in the far ultraviolet region. The reflectance remains high across the visible spectrum and begins to display absorption bands in the near infrared.

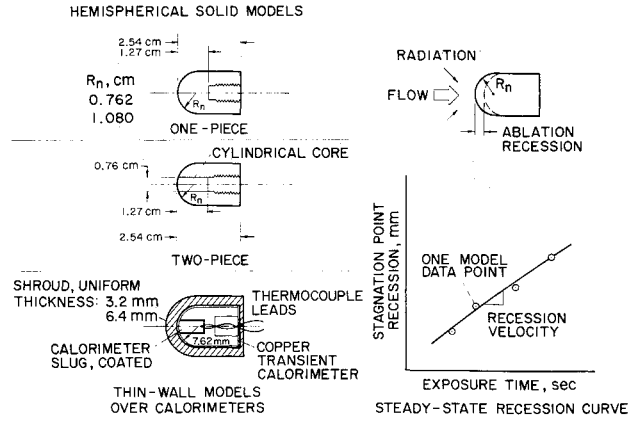

Fig. 4 Models and experimental procedure.

Tests, Ablation Models, Facility, and Experimental Procedure

Several types of tests were performed and a variety of measurements made to study the reflectance and performance of Teflon and boron nitride undergoing ablation. Surface recession rates were obtained in convective heating alone, radiative heating alone, and combined convective and radiative heating on both solid ablation models and thin-walled ablation models. Sketches of the shapes of the models used are shown in Fig. 4. Only the one-piece ($Rn = 0.762$ cm) model shape was used in the boron nitride tests. While the thin-walled Teflon models were undergoing ablation, the heat flux at the back face was determined by a transient-type calorimeter that was also used as a model support. The reflective efficiency of boron nitride prevented evaluation of radiative transmission using the thin-walled model tests. Surface brightness temperatures of ablating specimens were measured by a recording monochromatic pyrometer with a bandpass centered at 0.8 μ. For the boron nitride tests, a chopping device was used to periodically interrupt the entire incident radiation-beam for 3–5 msec duration approximately 20 times per sec. During this interval the pyrometer measurement consists solely of the surface brightness temperature since the reflected radiation is removed. An approximate indication of the in-situ model reflectivity can also be obtained when comparing the blocked and unblocked brightness levels. This set of testing techniques has proven valuable for theoretical evaluation of the material as a reflecting ablator and for assessing the optical properties during environmental exposure.

The ablation tests were performed in the Ames Advanced Entry Heating Simulator.[11] This facility is capable of subjecting test samples to either intense radiative heating alone or convective arc jet heating alone, or to both types of heating simultaneously. The test models were sequentially inserted one at a time into the heating environment for different lengths of time. Four models were usually tested. The thickness of the ablation specimens was measured at the stagnation point after the test and compared to the prerun measurement to determine the surface recession. For each model the surface recession measurement was plotted against time. The slope of these linear curves gave the surface recession velocity and the mass removal rate (Fig. 4).

For the thin-walled models the transient calorimeter was coated with a black coating and the heat flux was measured at the back surface of the thin-walled shroud as a rise in slug temperature. The stagnation-point cold-wall convective-heating rate was measured by a water-cooled steady-state calorimeter and by several copper transient calorimeters, identical to those used for the thin-walled ablation model tests. The stagnation point pressure was determined from a pitot pressure probe. The radiative heating rate was also measured with the steady-state calorimeter that was calibrated before the ablation tests in a radiation-only environment. The axial position of the calibration instruments or the ablating nose of the models is continuously maintained at a fixed common position during test exposure by using a laser optical device described in Ref. 11. This ensures that the calibration instruments measure the heating rate and pressure actually experienced by the model. Furthermore, the technique ensures that the model experiences a fairly constant heating flux and that the pyrometer continuously observes only the stagnation region of the model nose despite possible recession of the model surface due to ablation.

Results and Discussion—Teflon Tests

The Teflon material was studied first and will be discussed initially to demonstrate the potential of radiation reflection. The solid Teflon models were first subjected to convective heating alone. These results were compared with published theoretical predictions,[12,13] which used an empirical heat of ablation, to establish the validity of the convective test results. Excellent agreement between the measured and predicted values for convective heating was obtained for stagnation-pressures from 0.11 to 0.48 atm and cold-wall heating rates from 500 to 1000 w/cm^2 in air. Measurements of the surface brightness temperature at the stagnation region on the model were very low in accord with the low-melting point of Teflon.

Radiation-heating was superimposed upon the models for five of the convective conditions. The radiative heating varied from 1000 to 1400 w/cm^2. The surface recession for the combined convective-radiative heating tests and the corresponding convective-only tests is shown in Fig. 5. Three characteristic cases are shown that cover the pressure range and the two heating rate ranges. In all cases, the superposition of the radiative heating does not affect the material ablation rate over that observed for convective-only testing. The differences between the convective-only and the combined heating results are primarily due to experimental errors encountered in measurement accuracies and the use of a two-piece model as described in Ref. 5. Experimental error bars are shown for a single data point for each condition. The important point is that the slope of the curves at each condition remains unchanged when radiative heating is added to the convective condition. In other words, no additional surface recession resulted from doubling and tripling the imposed heating rate as a result of adding a radiative component. The surface brightness temperature of the models exposed to radiative heating was measured by the pyrometer and was in excess of 4000 K. Since the ablation rate remained unchanged and since the Teflon decomposes into gaseous products at about 760 K, these observations can only be explained on the basis of reflection of the radiation from the model (i.e., the pyrometer was viewing the reflected source radiation). The reflective property of Teflon (backscattering by the crystalline zones in the absence of absorption) prevents further material degradation. Recent calculations[14] indicate that the finite, though small, absorption coefficient for Teflon may ultimately lead to local internal degradation due to the large volume of material used to accomplish reflection, the focusing effect of the small models, and low dissipative conduction for Teflon. For the heating rates of these tests, conducted within the exposure times leading to possible internal failure, the surface recedes at the same rate as the thermal conductive front advances into the material (i.e., steady-state ablation is achieved). This is a consequence of the low thermal conductivity and low heat of sublimation for Teflon. Thus, the material remains reasonably cool in depth, maintaining its crystalline structure. If the material became translucent in depth ($T > 327$ C), the radiation would be transmitted rather than backscattered and would indicate a lower apparent surface brightness temperature.

Shrouded Calorimeters

To further ensure that the radiation was not simply being transmitted through the solid Teflon models or that the results were not dependent on model geometry, thin-walled Teflon

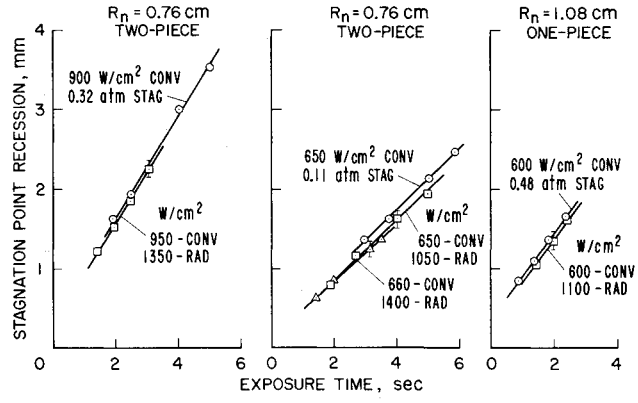

Fig. 5 Comparison of white Teflon at three convective-conditions and under combined convective-radiative heating conditions.

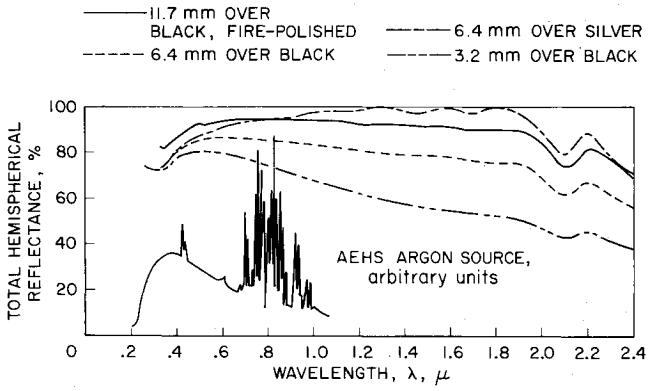

Fig. 6 Relation of source spectrum and spectral reflectance of Teflon.

shrouds over calorimeters were exposed to combined convective and radiative heating. These thin-walled ablation models were subjected to the same combined heating conditions as were used in the solid model tests. The transient calorimeter surfaces inside the Teflon shrouds were coated with a black coating to increase their absorptivity. Postrun measurements of the surface recession were compared with the solid-model data under corresponding conditions and showed excellent agreement. The heating fluxes measured at the calorimeter for Teflon shrouds 3.2 mm thick were 22 to 26% of that incident on the Teflon at the stagnation point. For shrouds 6.4 mm thick, the heating rate measured was about 10 to 16% of the incident flux at the ablation surface. These values are in excellent agreement with the values predicted from the total hemispherical reflectance measurements over the wavelength region of the arc radiation source shown in Fig. 6. The values of heating fluxes also compare favorably with a theoretical two-flux radiation transport model, using the Kubelka-Munk scheme, recently developed by Weston.[15] Most of the radiation transmitted to the calorimeters would be in the red and near infrared portion of the spectrum. The apparent surface brightness temperature observed was characteristically high. These measurements indicate that Teflon retains its crystalline feature during the ablation test and validates the application of the room temperature reflectance measurements to obtain approximate values for scattering and absorption to predict the radiation transport during combined testing. Further evidence that Teflon remains reasonably cool for the duration of these tests was provided by several shrouded calorimeters exposed to convective-only testing. No temperature rise was recorded at the calorimeter for 4-sec exposures, which indicates that the heating flux observed by the shrouded calorimeters during the combined tests was strictly due to radiation transport rather than conduction.

Each of these tests indicates the potential of reflecting almost all of the incident radiation of the gas cap away from the body. For example, white Teflon was compared to black Teflon (35% graphite pigmented) under nearly identical heating environments (Fig. 7). While the recession rates for white and black Teflon under convective-only conditions are nearly the same,

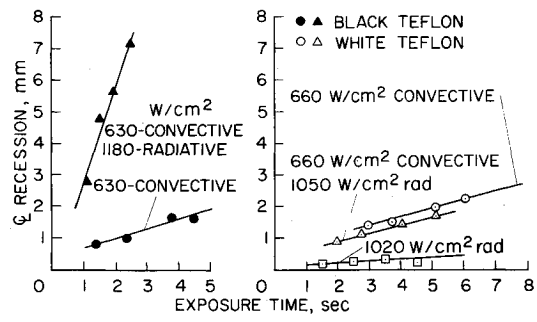

Fig. 7 Comparison of white and black Teflon under convective and radiative heating conditions.

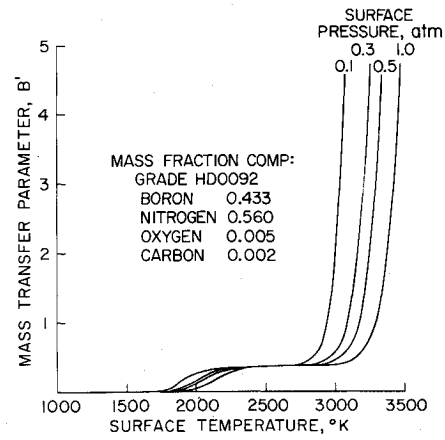

Fig. 8 Theoretical surface equilibrium mass transfer for boron nitride in an air boundary layer.

the rates for combined heating are markedly different. White Teflon displays the characteristic feature of reflectance with no change in surface recession, whereas the black Teflon recedes at nearly five times the convective-only rate. Obviously, absorption of the incident radiation seriously degrades the performance of black Teflon. Also shown on this figure is the recession of white Teflon under radiation-only testing in which very little recession occurs because the majority of the radiation is being backscattered out of the material. The slight degree of recession is probably due to the absorption in the near u.v. indicated in Fig. 6.

Test Results and Discussion—Boron Nitride

Boron nitride was investigated to illustrate a material that combines a higher sublimation energy (than Teflon) with reflectance. Boron nitride, much like graphite, sublimes at a relatively high temperature. The sublimation energy is over an order of magnitude greater than Teflon. In addition, at room temperature boron nitride has a high reflectance (Fig. 3) especially in the visible spectrum. At elevated temperatures, however, the optical properties of dielectric materials may differ considerably from the room-temperature properties. This may be due, in part, to excitation of the electronic states of the solid or to chemical phase or reaction changes on the surface of the material.

The theoretical thermochemical behavior of boron nitride in an air stream is shown in Fig. 8. A nondimensional mass transfer parameter (B') is plotted for a family of surface pressures against the surface temperature. The parameter is obtained by dividing the surface mass loss rate (m_s) by the transfer coefficient ($\rho_e u_e C_H$), obtained for stagnation point convective heat transfer in the presence of blowing. The lines in Fig. 8 are obtained from a thermochemical equilibrium program[16] that considered a film coefficient model for diffusion and minimized the free energy for the contributing species in the equilibrium mixture. The equilibrium mixture was taken for a control volume adjacent

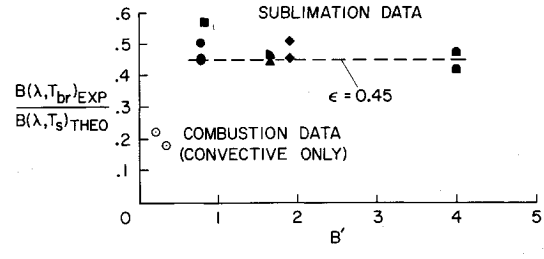

Fig. 9 Comparison of the experimental brightness level observed to the brightness level computed from the theoretical temperature for the same mass transfer parameter (B'); $B(\lambda, T)$ = Plancks' function.

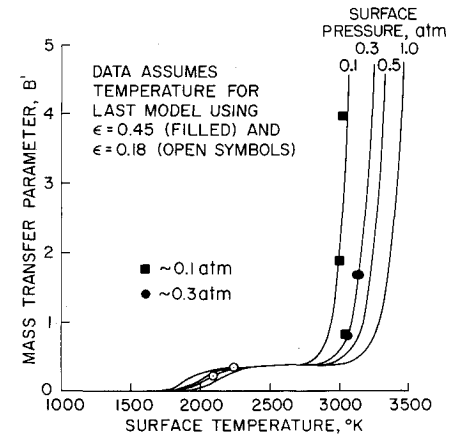

Fig. 10 Boron nitride performance under convective-only and combined convective-radiative heating.

to the surface whose temperature was identically equal to the surface temperature. For a given B' and a given surface pressure, the program specified a surface temperature and the mole fraction of each species contributing to the control volume mixture. The thermodynamic properties were obtained from the JANAF tables.[17] Three important regimes can be identified in the mass removal of boron nitride in air. The plateau of fairly constant B' (≈ 0.35) over a range of temperature primarily between about 2000 and 3000 K likely corresponds to surface combustion to form the oxidation product, B_2O_2. This regime is diffusion-limited by the availability of free oxygen. The liberated nitrogen forms molecular nitrogen. As the mass removal increases near the knee of the curves, the program predicts that the more stable product, BO is formed. The oxygen abundance is depleted in this regime as B' increases and the boron nitride begins to sublime into free boron and molecular nitrogen. The availability of oxygen is reduced by convective blockage. The rapid rise in B' with temperature in the 3000 K region is characterized by sublimation of the boron nitride, becoming a function of the surface pressure.

In the experimental evaluation of boron nitride, two types of testing were performed. Convective-heating-only tests were used to investigate the diffusion-limited plateau, then radiative heating was superimposed to drive the surface reactions into the sublimation regime. The intent of this initial testing was to investigate the effect of high-temperature ablation on the in-situ optical properties of boron nitride. An experimental grade (Union Carbide HD0092) of boron nitride was used because of its low oxygen content to help prevent spallation. The test conditions for the boron nitride tests were nearly the same as those of the Teflon tests.

The surface optical properties change when oxide reactions begin to form and the mass removal corresponds to a value of B' on the plateau. The surface acquires a light gray color (in contrast to the room temperature whiteness) characterized by an increased emissivity and a reduced reflectivity. Optical measurements (e.g., pyrometry) of the surface temperature of white materials is hampered considerably by their "whiteness", which may undergo significant variation in the course of a test exposure. The pyrometer and radiation chopper described earlier were used to measure the surface brightness temperature at the stagnation point. Without the chopper, the pyrometer records the sum of both the surface emission and the reflectance of the imposed radiation. With the radiation blocked (for short intervals) by the chopper, the brightness energy observed by the pyrometer is solely a function of the surface brightness temperature and the emissivity. For the B' measured in the test, a theoretical surface temperature can be obtained from Fig. 8. The ratio of observed surface brightness energy to the brightness energy computed from the theoretical temperature (assuming an emissivity of one) is plotted in Fig. 9 against the B'. For each B', more than one data point can be shown since this ratio can be formed for each model exposed whereas three or four exposures are required to obtain a recession velocity and hence, B'. This figure indicates that at low temperature (i.e., the convective-only results), the ratio is about 0.18, which is approximately equal to the spectral emissivity at 0.8 μ shown in Ref. 10. For data points in the sublimation regime, the ratio is fairly insensitive to B' over the range tested and is approximately equal to 0.45. Assuming an emissivity of 0.45, the measured surface brightness temperature can be corrected for each test condition. Figure 10 shows the corrected data points obtained, plotted on the theoretical B' curves described previously. Only the surface temperature for the final model in the four-model test sequence is shown at each condition. The convective-only tests (open symbols) are just into the diffusion limited regime of mass removal; whereas, the combined heating results (obtained by adding radiation to the convective conditions) drives the mass loss into the sublimation regime (filled symbols).

The increase in high-temperature emissivity must be accompanied by a corresponding decrease in reflectivity. For these measurements the reflectivity would appear to fall to 55% (i.e., one minus the emissivity) in the absence of transmissivity. The difference between the chopped (blocked incident radiation) and the unchopped (fully exposed radiation) brightness levels sensed by the pyrometer is a rough measure of the energy reflected from the surface. By comparing this difference at the beginning of the model exposure [when the reflectivity is known and diffuse (Fig. 3)] with the difference at the conclusion of the test (when the surface is at an elevated temperature and subliming), a ratio can be formed for surface reflectivity under subliming conditions. From the experimental data, this measurement indicates a reduction of the room-temperature reflectance in the visible from about 90 to about 55%. This value compares well with that indicated above even though the nature of the reflectivity has changed. In general, the change of surface shape and texture, and of surface properties due to sublimation and chemical phase changes would be expected to alter the angular dependence of the energy reflected from the model surface. In any case, the reflectivity of boron nitride is reduced in the presence of sublimation at high temperature. In particular, the reflectivity of boron nitride at high temperature is probably due to a combination of volumetric (e.g., backscattering) processes modified by surface effects such as phase changes (melting) or reaction changes (sublimation or oxidation products on the surface). Postrun observations of a model surface that had undergone sublimation have been obtained using a scanning electron microscope. The surface appears identical to Fig. 2, with no evidence of a heavy overcoating of metallic boron on the surface. The reflectivity probably remains highly diffuse although individual crystals may have free boron on their surfaces. In the subsequent discussion of applications, the performance for boron nitride will be examined assuming a reflectivity of 55%.

Application to Planetary Entries

The significance of reflecting incident radiation from the heat shield can be illustrated for the Venusian entry case. A parametric family of curves of different reflectivities (R) and convective blockage factor with asymptote of ($\psi = 0.1$ or 0.0) are shown in Fig. 11. The fraction of total entry mass (M_E) lost to ablation (M_L) during entry is plotted against the heat of sublimation (Δh). The entry body configuration is a spherical segment of nose radius, 32.3 cm, with a 45° half-angle cone afterbody as shown in the inset. The total probe mass is 22.7 kg. The entry begins at a velocity of 12.2 km/sec at an entry angle of 40°. The radiation heating pulse peaks at about 5 kw/cm^2, which is about 50% greater than the peak of the convective heating pulse. A combination of a reasonably high reflectivity and a high sublimation energy leads to a very low mass loss fraction, as does high sublimation energy alone. The value of reflection becomes more prominent with entries more strongly dominated by radiation (e.g., the Jovian entry case). For a low sublimation energy, Teflon for example ($\Delta h \approx 2$ MJ/kg), the effect of reflec-

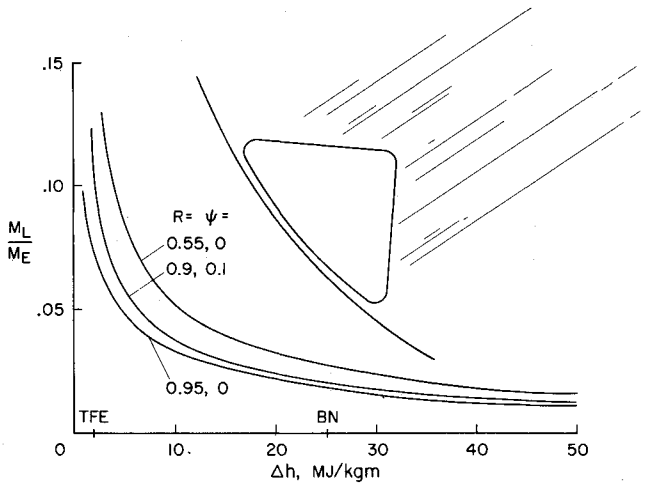

Fig. 11 Mass loss for Venusian entry vs heat of sublimation and reflectivity.

tance is pronounced and a 10% loss of mass would be experienced if the reflectance were 0.9 (and $\psi = 0.1$). For higher sublimation energies, quartz ($\Delta h \approx 13\ MJ/kg$), the mass loss is only about 3% for $R = 0.90$; whereas for materials like boron nitride ($\Delta h \approx 25\ MH/kg$), the mass loss remains about 3% despite an assumed reduced reflectance of 55%. Note that this loss of reflectivity for boron nitride creates nearly a 50% increase in mass loss at 90% reflectance, but the offsetting high sublimation energy maintains the mass loss at a low level.

The entry history for a boron nitride heat shield is shown in Fig. 12 for a Venus entry probe. The body configuration is described above. For an entry angle of 40°, an Allen-Eggers trajectory analysis,[18] predicts a peak radiative heating pulse of 5 kw/cm^2 after allowing for gas phase absorption in the boundary layer. The convective pulse, after convective blockage, peaks at about 3.5 kw/cm^2. The vehicle mass loss is about 3% for a reflectivity of the surface of 55%. If a safety factor of 2 were applied to a boron nitride heat shield, 6% of the entry mass would be required for thermal protection. However, boron nitride sublimes at a relatively high temperature so the payload for a Venusian entry probe would have to be insulated thermally from the high back face temperature of the heat shield. Studies of Venus entry probes utilizing charring ablators (Ref. 19) indicate a thermal protection fraction of 10%. The additional mass required for insulation from a boron nitride heat shield would probably balance the remaining 4% difference. The competitive fraction required for a boron nitride heat shield would make a reflective heat shield on the Venusian mission an attractive prelude to future missions with more severe radiative environments.

The Jovian entry case presents a more remarkable demonstration of the advantage of reflection by the heat shield. The magnitude of the radiative heating pulse may increase by tenfold in some cases whereas the convective heating may double. In

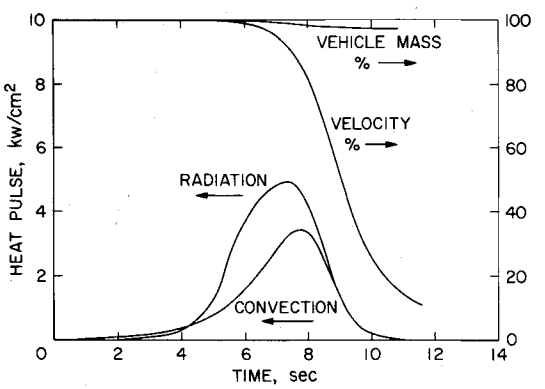

Fig. 12 Venusian entry history with a boron nitride heat shield.

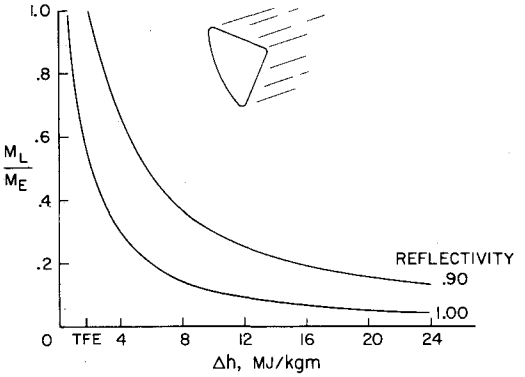

Fig. 13 Mass loss for Jovian entry vs heat of sublimation and reflectivity.

Ref. 5 a Teflon heat shield, considered to reflect all of the incident radiation in accord with the results presented above, was investigated for Jovian entry. Since the radiation was considered to be reflected, the heating consisted of convection only. A blunt-nose shape was used to reduce the convective heating load. Nevertheless, an Allen-Eggers trajectory analysis indicated a convective pulse peak of 9 kw/cm^2 that was then reduced by convective blockage[20] to about 2 kw/cm^2. The radiative pulse peaked at 56 kw/cm^2 after allowing for gas phase absorption. The surviving mass fraction was computed to be 47%. This is comparable to the level of mass loss predicted for a graphitic heat shield[2] in spite of the very low heat of sublimation of Teflon (1.74 MJ/kg) compared to graphite (23 MJ/kg). The intrinsic advantage of combining the reflectance of radiation with the blunting of the body to reduce convective heating is at once apparent.

Furthermore, combining a higher heat of sublimation with reflectance produces the same effect on mass loss for Jovian entry as for Venus entry. The reducing effect for Venus is completely analogous for Jovian entry as shown in Fig. 13. The entry body configuration is a spherical segment of nose radius, 0.8 m, with a 60° half-angle cone afterbody as shown in the inset (i.e., the body of Ref. 2 turned around). The total probe mass is 250 kg. The entry begins at 50 km/sec at an initial entry angle of 15°. The heating pulses are indicated previously. The value of reflection becomes evident at once, especially when combined with higher sublimation energies.

Conclusions

The principle of a reflecting/ablating heat shield has been demonstrated for two widely different materials, Teflon and boron nitride. Teflon is not considered a prime candidate for heat shield systems for the planetary missions, but it effectively illustrates the principle of diffuse reflection from a heat shield. Boron nitride, in its present commercial solid form, is not necessarily recommended for heat shield material, but is intended to illustrate that a high heat of sublimation can be combined with reflectance. The important practical problem now is to develop improved dielectric materials that exhibit good reflective properties to respond to the radiatively dominated environments and yet act effectively as ablative heat shield systems.

The performance of the reflecting heat-shield was demonstrated for entry into the Venusian and Jovian atmospheres. A parametric study indicates that the combination of a reasonably high reflectance and a higher sublimation energy than Teflon can lead to significant reductions in mass loss due to ablation during entry. Despite the loss of reflectivity for boron nitride, the reflectivity that remains proves advantageous in a radiation-dominated entry environment as a means of energy accommodation. The mass loss history of a boron nitride heat shield for a Venusian entry case was illustrated. Radiation shielding by reflection permits the use of blunt entry configurations for purposes of reducing convective heating. Dielectric reflectors, which reject a substantial fraction of the imposed radiative heat-

ing in radiation environments, show promise of improved performance over heat shields made of opaque sublimers such as graphite.

References

[1] Wakefield, R. M. and Lundell, J. H., "Ablative Heat Shields for Jupiter Entry Probes," AAS Paper 71-146, *Proceedings of the 17th Annual Meeting of the American Astronautical Society*, June 28-30, 1971, Seattle, Wash.

[2] Tauber, M. and Wakefield, R., "Heating Environment and Protection During Jupiter Entry," *Journal of Spacecraft and Rockets*, Vol. 8, No. 6, June 1971, pp. 626-636.

[3] Jaworski, W. and Nagler, R.G., "A Parametric Analysis of Venus Entry Heat-Shield Requirements," TR 32, 1970, NASA.

[4] Allen, H. J., "Gas Dynamics Problems of Space Vehicles," Proceedings of the NASA/University Conference on the Science and Technology of Space Exploration, Nov. 1-3, 1962, Chicago, Ill.

[5] Nachtsheim, P. R., Peterson, D. L., and Howe, J. T., "Reflecting Ablative Heat Shields for Radiative Environments," AAS Paper 71-147, 1971, also; *Proceedings of the 17th Annual Meeting of the American Astronautical Society*, June 28-30, 1971, Seattle, Wash.

[6] Kirker, M., *The Scattering of Light and Other Electromagnetic Radiation*, Academic Press, New York, 1969, Chap. 4.

[7] Sears, F. W., *Optics*, Addison-Wesley, Reading, Mass., 1949, pp. 364-365.

[8] Sperati, C. A. and McPherson, J. L., "The Effect of Chrystallinity and Molecular Weight on Physical Properties of Polytetrafluoroethyline," *Proceedings of the American Chemical Society Meeting*, Atlantic City, N. J., Sept. 1956.

[9] Edwards, D. K., Gier, J. T., Nelson, K. E., and Roddick, R. D., "Integrating Sphere for Imperfectly Diffuse Samples," *Journal of the Optical Society of America*, Vol. 51, No. 11, Nov. 1961, pp. 1279-1288.

[10] *Thermophysical Properties of High Temperature Solid Materials*, Vol. 5, edited by V. S. Touloukian, Purdue Univ., Lafayette, Ind., Macmillan, New York, 1967.

[11] Peterson, D. L., Gowen, F. E., and Richardson, C. L., "Design and Performance of a Combined Radiative Convective Heating Facility," AIAA Paper 71-255, Albuquerque, N. Mex., March 1971.

[12] Heister, N. K., and Clark, C. F., "Feasibility of Standard Evaluation Procedures for Ablating Materials," Rept. 8, May 1965, Stanford Research Inst., Menlo Park, Calif.

[13] Fay, J. A. and Riddell, F. R., "Theory of Stagnation Point Heat Transfer in Dissociated Air," *Journal of the Aeronautical Sciences*, Vol. 25, No. 2, Feb. 1958, pp 73-85.

[14] Howe, J. T. and Green, M. J., "Thermal Shielding by Subliming Volume-Reflectors in Convective and Intense Radiative Environments," *AIAA Journal*, to be published.

[15] Weston, K., "Scattering for Materials with Densely Packed Scattering Centers," oral presentation at the Symposium on Hypervelocity Radiating Flow Fields for Planetary Entries, JPL, Pasadena, Calif., Jan. 1972, also; private communication.

[16] McCuen, P. A., Schaefer, J. W., Lundberg, R. E., and Kendall, R. M., "A Study of Solid Propellant Rocket Motor Exposed Materials Behavior, Final Report," Contract AF Or(611)09073, Feb. 26, 1965, Vidya Div. Itek Corp. Palo Alto, Calif.

[17] *JANAF* Thermochemical Tables and Supplements to 1966, Dow Co., Midland, Mich.

[18] Allen, H. J., and Eggers, A. J., "A Study of the Motion and Aerodynamic Heating of Ballistic Missiles Entering the Earth's Atmosphere at High Supersonic Speed," Rep. 1381, 1958, NACA.

[19] *Planetary Explorer Universal Bus Study*, AVCO Corp. Final Rep., NAS5-11800 mod. 2, Oct. 1970, Lowell, Mass.

[20] Lundell, J. H., Winovich, W., and Wakefield, R. W., "Simulation of Convective and Radiative Entry Heating," Second National Symposium of Hypervelocity Techniques, March 1962, Denver, Colo.

NOVEMBER 1972 AIAA JOURNAL VOL. 10, NO. 11

Investigation of Simulated Melting Instability Waves Near Stagnation Region in Hypersonic Flow

WILLIAM KUZYK* AND CHING JEN CHEN†

University of Iowa, Iowa City, Iowa

Melting waves in hypersonic flow were simulated at room temperature with parabolic frozen oil models for gas Reynolds number, N_{Reg}, 15,000 to 37,000, liquid Peclet number, β, 1 to 10^{-3}, for inverse Froude number, G, 1 to 7, and for gas Prandtl number of order one. Results show that Kelvin-Helmholtz instability waves were generated at $N_{Reg} < 25{,}000$ and $\beta < 0.005$, shear instability waves at $N_{Reg} < 25{,}000$ but at $\beta > 0.005$. Three-dimensional waves were observed at an approximate increase of 5000 in gas Reynolds number. Inclusion of high temperature data of quartz and Tektite agreed with the simulated wave pattern.

Nomenclature

A = acceleration in ft/sec^2
C = $\omega\lambda/U_\infty$ nondimensional wave velocity
ω = the number of waves generated per second
U_∞ = wind velocity, fps
L = R, radius of model, in ft
ρ_g = density of air, slugs/ft^3
ρ_l = density of liquid, slugs/ft^3
C_{pg} = specific heat, Btu/slug °R
μ_g = viscosity of gas, slugs/ft sec
K_g = thermal conductivity Btu/ft sec °R
P_{rl} = $C_{pl}\mu_l/K_l$ liquid Prandtl number
C_{pl} = specific heat for liquid, Btu/slug °R
μ_l = viscosity of liquid, slugs/ft sec
K_l = thermal conductivity of liquid, Btu/ft sec °R
Λ = λ/R nondimensional wavelength
λ = wavelength, ft

Presented as Paper 72-92 at the AIAA 10th Aerospace Sciences Meeting, San Diego, Calif. January 17-19, 1972; submitted February 14, 1972; revision received June 9, 1972.

Index categories: Material Ablation; Thermal Modeling and Experimental Thermal Simulation; Boundary-Layer Stability and Transition.

* Graduate Student, Department of Mechanical Engineering.

† Associate Professor, Department of Mechanical Engineering and Research Engineer, Institute of Hydralic Research. Member AIAA.

Introduction

ONE of the aerodynamic features of re-entry and entry vehicles through any atmosphere may be the melting ablation in the stagnation region of hypersonic flow. The melting waves generated at the gas-liquid interface play an important role in flight dynamics as well as the heat transfer characteristics. High-temperature tests of such hypersonic flow is a costly task and it is rather difficult to make detailed observations of the type of melting waves present. Conversely an approximated low-temperature simulation can be achieved at a lower cost and provides a longer experimental duration and observation of actual motion of melting waves.

Chen and Ostrach[1] showed a close similarity between simulated melting ablation experiments in a deceleration field using frozen oil model and the actual Tektites described and shown by Chapman.[2,3] In fact when right similarity parameters are simulated the forward portion of the perimeter wave was very similar in appearance of wave spacing and wave amplitude. They also suggested that melting pattern near the stagnation region in the hypersonic flow may resemble that of water waves generated on a thin film as investigated by Craik.[4] Craik showed the existence of slow waves that correspond to Kelvin-Helmholtz instability waves and the existence of fast waves that correspond to the shear instability waves. The slow (fast) wave is defined